The American Journal of Pathology, Vol. 172, No. 1, January 2008
Copyright © American Society for Investigative Pathology
DOI: 10.2353/ajpath.2008.070130

Cardiovascular, Pulmonary and Renal Pathology

Regulation of Endothelial Cell Cytoskeletal Reorganization by a Secreted Frizzled-Related Protein-1 and Frizzled 4- and Frizzled 7-Dependent Pathway

Role in Neovessel Formation

Pascale Dufourcq,* Lionel Leroux,*† Jérome Ezan,* Betty Descamps,* Jean-Marie Daniel Lamazière,* Pierre Costet,‡ Caroline Basoni,§ Catherine Moreau,* Urban Deutsch,¶ Thierry Couffinhal,*† and Cécile Duplàa*

From INSERM U828, Pessac, France; the Centre de Transgenose,‡ Université Victor Ségalen Bordeaux 2, Bordeaux, France; the Department of Cardiology,† Hôpital Haut Lévêque, Pessac, France; Institut Européen de Chemie et Biologie (IECB),§ Pessac, France; and the Theodor Kocher Institute,¶ University Bern, Bern, Switzerland*

Consistent with findings of Wnt pathway members involved in vascular cells, a role for Wnt/Frizzled signaling has recently emerged in vascular cell development. Among the few Wnt family members implicated in vessel formation in adult, Wnt7b and Frizzled 4 have been shown as involved in vessel formation in the lung and in the retina, respectively. Our previous work has shown a role for secreted Frizzled-related protein-1 (sFRP-1), a proposed Wnt signaling inhibitor, in neovascularization after an ischemic event and demonstrated its role as a potent angiogenic factor. However the mechanisms involved have not been investigated. Here, we show that sFRP-1 treatment increases endothelial cell spreading on extracellular matrix as revealed by actin stress fiber reorganization in an integrin-dependent manner. We demonstrate that sFRP-1 can interact with Wnt receptors Frizzled 4 and 7 on endothelial cells to transduce downstream to cellular machineries requiring Rac-1 activity in cooperation with GSK-3β. sFRP-1 overexpression in endothelium specifically reversed the inactivation of GSK-3β and increased neovascularization in ischemia-induced angiogenesis in mouse hindlimb. This study illustrates a regulated pathway by sFRP-1 involving GSK-3β and Rac-1 in endothelial cell cytoskeletal reorganization and in neovessel formation. ***(Am J Pathol 2008, 172:37–49; DOI: 10.2353/ajpath.2008.070130)***

The formation of new blood capillaries is an important component of pathological tissue repair in response to ischemia. This angiogenic process is complex, involving endothelial cell (EC) movement and proliferation, requiring spatial and temporal coordination of multiple angiogenic factors, receptors, intracellular signaling pathways, and regulatory factors. Although the early phases of capillary tube formation have been well studied, the final steps of endothelial tube organization remain elusive. Extracellular signals may be involved in regulating endothelial cell morphology through changes in the cytoskeleton organization. Recently, the Wnt proteins and their Frizzled (Fzd) receptors have emerged as an integrative system of extracellular signals within intracellular pathways that regulates blood vessel formation.

The secreted Wnt proteins (19 members in mouse)[1] activate canonical and noncanonical signaling pathways by binding to two types of receptors: Frizzled proteins (Fzd) (10 structurally related proteins in mouse)[2] and lipoprotein LRP-5/6 receptors.[3] The canonical pathway involves nuclear translocation of the β-catenin, which

Supported by The European Vascular Genomics Network (grant 503254), the Fondation de France (grant 2006005678), the Groupe de Réflexion pour la Recherche Cardiovasculaire (to L.L.), and the Fondation pour la Recherche Médicale (to L.L.).

P.D., L.L., and J.E. contributed equally to this study.

Accepted for publication October 2, 2007.

Supplemental material for this article can be found on *http://ajp.amjpathol.org.*

Current address of J.E.: Mount Sinai School of Medicine, Molecular, Cell and Developmental Biology Department, New York, NY.

Address reprint requests to Cécile Duplàa, INSERM U828, Av du haut lévèque, 33600 Pessac, France. E-mail: cecile.duplaa@bordeaux.inserm.fr.

forms complexes with the TCF/LEF-1 transcription factors and activates the expression of various genes.[4] The noncanonical pathway implicates the cell polarity pathway (PCP), which guides cellular movements during gastrulation, and the Wnt/Ca^{2+} pathway as evidenced in *Xenopus* and Zebrafish.[5] The Wnt pathway antagonists can be divided into two functional classes: the sFRP family and the Dickkopf protein family.[6] The sFRP proteins are able to bind either to the Wnt ligands or to the Fz receptors.[7]

Genetic studies in mice have provided insights into the knowledge of Wnt/Fz molecular players that regulate the growth of blood vessels in the embryo. Following are a few examples of the consequences of the inactivation of those molecular factors. Inactivation of *Fzd5* alters vessels in the yolk sac and in the placenta of the embryo.[8] Inactivation of the *Fzd4* gene reveals a malformation of the secondary and tertiary retinal vascular network.[9] Inactivation of the *Wnt2* gene causes alterations of the placenta formation.[10] Mice with a deletion of the *Wnt7b* gene display altered hemorrhagic vessels in the lung.[11] In the adult, activation of the Wnt signaling pathway has been observed in newly formed vessels.[12,13] The mechanisms by which Wnt signaling is involved in vessel formation are not obvious. The Wnt factors are known to activate a β-catenin-dependent pathway, inducing transcription of target genes capable of stimulating vessel formation, ie, cyclin D1, c-*myc*, MMP7, and vascular endothelial growth factor. In previous studies, we have shown that sFRP-1 overexpression, during the early phase of angiogenesis, impedes the β-catenin pathway and delays vascular cell proliferation.[14] We have also demonstrated that sFRP-1 favored EC migration and differentiation, protected ECs from apoptosis *in vitro*, and led to a robust vessel formation in different angiogenic models (eg, tumoral, plug, chorioallantoic membrane assays).[15] Its role in vessel formation remains to be elucidated.

In this study, using genetic and biochemical approaches, we have begun a molecular characterization of an unexplored β-catenin-independent Wnt/Fzd signaling pathway functioning in ECs through Fzd receptors and Rac-1. Our findings demonstrate that sFRP-1 is essential to the regulation of EC spreading as revealed by an increase in EC focal contact and actin stress fiber formation in a GSK-3β- and Rac1-dependent manner. Furthermore, *Fzd4* and *Fzd7* depletions phenocopy sFRP-1-induced EC spreading, revealing that sFRP-1 could regulate the endothelial cell spreading through Fzd4 and Fzd7 blockade. *In vivo*, EC-specific overexpression of sFRP-1 in transgenic mice blocked inactivation of GSK-3β and consequently increased neovascularization in ischemia-induced angiogenesis in mice.

Materials and Methods

Endothelial Cell Culture and Transfection

Human umbilical vein endothelial cells (HUVECs) from Clonetics were cultured in EBM-2 complete medium with EGM2 single coat (Clonetics). Porcine aortic endothelial cells (PAECs) were cultured in F-10 medium supplemented with 10% heat-inactivated fetal calf serum, 2 mmol/L L-glutamine, and penicillin-streptomycin. MS1 murine endothelial cells, a generous gift from Dr. Arbiser (Emory University, Atlanta, GA),[16] were cultured at 33°C in Dulbecco's modified Eagle's medium supplemented with 5% fetal calf serum (Gibco BRL), 1 mmol/L sodium pyruvate, and penicillin-streptomycin. PAE cell lines expressing N17 Rac under the control of an isopropyl-β-D-thiogalactopyranoside (IPTG)-inducible promoter were established previously[17] and cultured in the same medium supplemented with 100 μmol/L hygromycin B (Calbiochem) and 500 nmol/L puromycin (Calbiochem). Expression was achieved by 5 mmol/L IPTG for N17 Rac-expressing cell lines. Because the recombinant bovine FrzA protein[18] is almost identical to its homologous murine sFRP-1 protein (98% of identity), we chose here to rename FrzA to recombinant bovine sFRP-1 protein (rb sFRP-1). In all experiments, cells were activated with 10 nmol/L estimated rb sFRP-1 protein. Transfections were performed using Lipofectamine (Invitrogen) according to the manufacturer's instructions. The plasmids harboring FzCRD-myc-GPI, mouse Fz4-HA, and Fzd7 were kindly provided by Dr. Jeremy Nathans (Johns Hopkins University, Baltimore, MD). The plasmid harboring rb sFRP-1-myc::his was described in Jaspard and colleagues.[19]

Cell Attachment and Spreading Assays

Assays were performed with glass slides[20] (Labtek-II system; Nalge Nunc International Corp.) coated with polylysine (PL), type I (Coll I) or type IV collagen (Coll IV), and laminin (LM) (Biosource), in phosphate-buffered saline (PBS) at 5 μg/cm^2. Cells in serum-free medium were incubated for 15 minutes with or without rb sFRP-1 and allowed to spread for 2 hours at 37°C. After fixation in 2% paraformaldehyde, and permeabilization (0.2% Triton X-100), cells were either stained with hemalun or rhodamine-phalloidin (Molecular Probes) or incubated with a vinculin antibody (Sigma) revealed by a secondary anti-mouse fluorescein isothiocyanate antibody (Beckman Coulter) to assess cell morphology and estimate cell spreading areas. Cell spreading results were expressed as the ratio of spread cells/total adherent cells for each field. Results were expressed as the mean ± SD of six random fields per counted well (four wells per condition). Each experiment was done in triplicate. Cell spreading area was quantified using Sigma Scan Pro Software (National Institutes of Health, Bethesda, MD). Results are expressed as μm^2.

The contribution of integrins to cell spreading was assessed using function-blocking mouse antibodies (Abs) as specified in the text at a concentration of 4 μg/ml: human αvβ3 (LM609), α2β1 (BHA2.1), and β1 (6S6) (Chemicon), and a mouse IgG (Sigma) as control. Cells were incubated in suspension with the described Ab for 15 minutes before starting the spreading assay. SB 216763 (10 μmol/L, Biomol), a GSK-3β inhibitor, was added 30 minutes before the initiation of the assay.[21]

Confocal Analysis

For immunolocalization of rb sFRP-1, CHO were seeded on glass slides (Labtek-II system, Nalge Nunc International Corp.) and transfected with plasmids harboring Fzd4-HA or Fzd7. Twenty-four hours after transfection, cells were incubated with rb sFRP-1-myc in 20 mmol/L Hepes, 140 mmol/L NaCl, 0.05% Tween 20 at 11°C for 1 hour, further rinsed with the same buffer, and fixed with 2% paraformaldehyde for 10 minutes at room temperature. After saturation in 5% bovine serum albumin with PBS for 1 hour, slides were incubated with an anti-c-*myc* antibody (1:1000; Upstate) overnight at 4°C, and revealed by a secondary anti-mouse biotinylated antibody. For the second staining, the slides were saturated with 5% bovine serum albumin for 1 hour, and further incubated with antibodies against either anti-HA (dilution, 1:1000; Santa Cruz Biotechnology) or anti-Fzd7 (1:1000; R&D Systems) overnight at 4°C, followed by fluorescent labeling with anti-rabbit or anti-goat Alexa Fluor 568 (Molecular Probes), respectively, for 30 minutes at room temperature. Fluorescence was examined with a confocal microscope (Nikon PCM 2000) using a 60×/1.4 Apoplan oil immersion objective. Fluorescein isothiocyanate/Alexa 568 channels were acquired by simultaneous scanning and images were analyzed with Imaris software (Bitplane AG). *Z*-stacks were performed with a step size of 0.4 μm.

Fluorescence-Activated Cell Sorting (FACS) Analysis of Integrin Expression

Expression of β1 subunit in HUVECs and PAECs was determined by flow cytometry. After a 16-hour serum starvation with 1% fetal calf serum and 0.5% bovine serum albumin, cells were incubated with rs FRP-1 for 4 and 16 hours. Cell flow cytometric analyses were performed on monodispersed endothelial cell suspensions prepared by brief incubation in 5 mmol/L ethylenediaminetetraacetic acid at 4°C as previously described.[14] Cells were incubated with anti-human β1 subunit antibody (1:1000; Tebu) for 1 hour at 4°C then with an fluorescein isothiocyanate goat anti-mouse IgG (Amersham) for 30 minutes. Samples were analyzed immediately in a fluorescence-activated cell sorter (FACS analyzer ODAM-ATC 3000).

Recombinant Adenovirus Infection

Different adenoviruses were used for functional studies. Cells in culture were infected at a multiplicity of infection of 100 with 1) adenoviral vectors expressing either β-galactosidase (Ad βgal), wild type (Ad GSK-3β-WT), constitutively active (Ad GSK-3β-S9A), and catalytically inactive (Ad GSK-3β-KM) forms of GSK-3β (kindly provided by Dr. K. Walsh, Boston University School of Medicine, Boston, MA)[22]; 2) Ad N17 Rac or Ad V12 Rac expressing a dominant-negative form (N17Rac) or a constitutively active (V12Rac) of Rac1, respectively, under the control of tetracycline repressor elements and a minimal CMV promoter (tet-mCMV) (gift from Dr. J.M. Bishop, University of California, San Francisco); 3) a virus constitutively expressing a tetracycline repressor-VP16 fusion protein, which was required to activate expression of the tet-mCMV.[23] For co-infection experiments, the first adenovirus infection was performed 6 hours before the second one. Recombinant adenoviral stocks were generated and provided by the vector core facility of Nantes' (France) University Hospital.[24]

Western Blotting

After cells were rinsed with cold PBS, they were lysed for 5 minutes in RIPA buffer (1% Nonidet P-40, 0.5% deoxycholate, 0.1% sodium dodecyl sulfate, 50 mmol/L Tris, pH 8.0, 1 mmol/L aprotinin, 1 mmol/L AEBSF, 1 mmol/L benzamidine, 1 mmol/L orthovanadate). Fifty μg of protein, quantified by bicinchoninic acid assay (Pierce) were separated by sodium dodecyl sulfate/polyacrylamide gel electrophoresis and transferred onto polyvinylidene difluoride membranes (Millipore). Membranes were incubated with the following antibodies: for the integrin activation, anti-phospho α-PAK and anti-α-PAK (Santa Cruz Biotechnology); for the Wnt/Frizzled pathway: anti-phospho-Ser9-GSK-3β (Cell Signaling), anti-total-GSK-3β (Cell Signaling), anti-β-catenin (Sigma), anti-phospho-ser9-β-catenin antibodies (Cell Signaling), anti-α tubulin (Sigma), anti-phospho-AKT (Cell Signaling) and anti-AKT (Cell Signaling); for Rac expression: anti-Rac1 (Pierce); for recombinant protein experiments, anti-His (Clontech), anti-Myc (Santa Cruz Biotechnology); for angiogenic factor expression: polyclonal antibodies against vascular endothelial growth factor, angiopoietin-1/2 (Santa Cruz Biotechnology). Binding of antibodies to the blots was detected using a chemiluminescence-enhanced chemiluminescence Western blotting system (Amersham). Relative protein levels were quantified using Scion software (Scion Corporation) on scanned films.

Rac Activity Assays

HUVEC and PAEC cultures grown to confluence were starved overnight in serum-free medium. Cells were incubated with rb sFRP-1 at 37°C for different periods of time (0, 10, 20, 30 minutes) and treated using the EZ-Detect Rac1 activation kit (Pierce) according to the manufacturer's instructions. Briefly, after lysis, cells were incubated with GST-human PAK1-PBD in the presence of a SwellGel immobilized glutathione disk. Proteins were separated by sodium dodecyl sulfate-polyacrylamide gel electrophoresis on 12% acrylamide gels before Western blotting with anti-Rac1 antibody. Before incubation with the beads, 10 μl were removed from all samples to control for equal loading of total Rac1. The amount of PAK-bound GTPase was normalized to the total amount of GTPase in the cell lysate for the comparison of GTPase activity (level of GTP-bound GTPase) in different samples.

Immunoprecipitation

Transfected CHO cells were washed with PBS, treated 30 minutes at 4°C with 4 mmol/L 3,3-dithiobis-sulfosuccinimidylpropionate (Pierce), washed three times with 50 mmol/L Tris-HCl buffer (TBS, pH 7,4), and detached from the plates with 5 mmol/L ethylenediaminetetraacetic acid/TBS. After centrifugation, the pelleted cells were lysed in buffer A (50 mmol/L Tris-HCl buffer, pH 7.4, 0.5% Nonidet P-40, 0.5% Triton, 1 mmol/L $CaCl_2$, 1 mmol/L $MgCl_2$, 2% glycerol, 150 mmol/L NaCl containing protease inhibitors) as described.[9] The insoluble fraction was removed and the supernatant incubated with anti-His microbeads (μMACS anti-His microbeads; Miltenyi Biotec). The samples were prepared following the manufacturer's instructions by sodium dodecyl sulfate-polyacrylamide gel electrophoresis, transferred to polyvinylidene difluoride membrane (Millipore), and probed with anti-Myc antibody (1:x, mAb 9E10; Santa Cruz).

Analysis of Frizzled RNA by Reverse Transcriptase-Polymerase Chain Reaction (RT-PCR) and RNA Interference Assay

Total RNAs were prepared from MS1 EC line in guanidinium thiocyanate buffer, and RT-PCRs were performed as previously described.[18] Negative controls without RT were prepared in parallel for each RNA sample. Semiquantitative PCR was performed as previously described.[25]

siRNA were either chemically synthesized for *Fzd 2*, *Fz 4*, and *Fzd 7* genes, (Ambion) or made for *Fz 5* and *Fz 6* genes by *in vitro* transcription using RNA silencer kit (Ambion). Two synthetic 21-nucleotide siRNAs per *Frizzled* gene were designed as follows (sense strand is given): Fzd 2#1, 5′-GGAAGUUCUACACUCGUCUTT-3′; Fzd 2#2, 5′-GCUAUAAGUUUCUGGGUGATT-3′; Fzd 4#1, 5′-GGACCAGGUGAUGAAGAGGTT-3′; Fzd 4#2, 5′-GGUGAUGAAGAGGUUCCCUTT-3′; Fzd 6#1, 5′-GGCUAUAGGUUUCUGGGAATT-3′; Fzd6#3, 5′-GGUUUUCUUAGAUACUUUGTT-3′; Fzd 7#1, 5′-GGUGCAGUGUUCUCCUGAGdTdT-3′; Fzd 7#2, 5′-GCCAUAUCACGGCGAGAAAdTdT-3′. *In vitro* siRNA synthesis has been described elsewhere.[26] The Fzd 5 siRNAs were produced by *in vitro* transcription using the Silencer siRNA cocktail kit. The PCR fragments for Fzd5 (using the following primers for Fzd5: sense 5′-AAGGAAGAGAAGGCGAGTGACC-3′ and antisense 5′-TAGGGCTGGAGGGATGATTAGG-3′; for Fzd6, sense 5′-TATCTCTGCGGTCTTCTGGGTTGG-3′ and antisense 5′-TCCATTGCTTCTCTCCTTCAGGC-3′) were purified (QIAquick PCR purification kit; Qiagen), subcloned into the vector pGEM-T (Promega) and sequenced. The resulting plasmids were used as templates to prepare siRNA cocktails corresponding to the individual genes according to the manufacturer's instructions. Briefly, 2 μg of linearized plasmid was *in vitro* transcribed by T7 RNA polymerase in a 20-μl reaction volume during 2 hours at 37°C. For annealing of siRNA duplexes, siRNA strands were heated for 5 minutes at 80°C and then slowly cooled to room temperature. Annealed siRNAs were assessed for double-stranded character by agarose gel (1% w/v) electrophoresis and ethidium bromide staining. Then, 15 μg of dsRNA for each gene of interest was digested with 15 U RNase III for 1 hour at 37°C. RNase III digests long dsRNA into short duplex products ranging from ~12 to 15 bp in length. A siGlo cyclophilin B siRNA (Dharmacon) was used as control. MS1 cells were seeded at a density of 20,000/cm^2 the day before transfection and they were ~40% confluent at the time of transfection. Transfection was performed in Lipofectamine (Invitrogen) according to the manufacturer's instructions. The following optimal siRNA concentrations were used: siRNA Fzd2#1, Fzd2#2, Fzd4#1, Fzd2#2 (100 nmol/L), siRNA Fzd7#1, Fzd7#2 (60 nmol/L), siRNA Fzd5 (40 nmol/L), and siRNA Fzd6 (80 nmol/L). Transfection medium was maintained on cells for 6 hours and then removed to be replaced by complete medium. Cells were used for experiments after 48 hours and Frizzled RNA silencing was assessed by RT-PCR to confirm knockdown using the following sense and antisense primers, respectively: Fzd1, 5′-GCAACCTACTTTCTTCCCCCTG-3′ and 5′-CGTGTTTGTCTCTCTCACCCATC-3′; Fzd2, 5′-TCAAGGTGCCGTCCTATCTCAG-3′ and 5′-GGTGGTGACCGTGAAGAAAGTG-3′; Fzd3, 5′-TGGGGTTTCTCTCCTTTTAGCC-3′ and 5′-GCTTTGCTTCTTTGGTCATCCACC-3′; Fzd4, 5′-TGACAACTTTCACGCCGCTCv, 5′-TACAAGCCAGCATCGTAGCCACAC-3′; Fzd5, 5′-CGTTGCCACCTTCCTCATTGAC-3′ and 5′-GCACCAAGAATCCCAGTGACAC-3′; Fzd6, 5′-TATCTCTGCGGTCTTCTGGGTTGG-3′ and 5′-TCCATTGCTTCTCTCCTTCAGGC-3′; Fzd7, 5′-TGTGTCTCTCTTTCGCATCCG-3′ and 5′-AACCATCTCTCGCCCCCAAATC-3′; Fzd8, 5′-CATCTGGTGGGTAATCCTGTCG-3′ and 5′-AGGTTGTCAAGGCTCTGGTTGC-3′; Fzd9, 5′-GAGCCTGTGCTACCGAAAAATG-3′ and 5′-CCTTCTGCCCCTTCTTATCCTG-3′; Fzd10, 5′-TGGTGTGTGTTATGTGGGCAGC-3′, 5′-ATCAGGCAGTCAGGTGTCTTGG-3′.

For quantitative analysis of sFRP-1 expression *in vivo*, 500 ng of total RNA from mouse tissues were reverse-transcribed; PCR was done using IQ SYBR Green supermix (Bio-Rad). An MJ Research Opticon and the following parameters were used for real-time PCR: 95°C for 5 minutes followed by 35 cycles of 95°C for 15 seconds, 60°C for 20 seconds, and 72°C for 15 seconds. Negative controls without RT were prepared in parallel for each RNA sample. All experiments were done in triplicate and differences in cDNA input were compensated by normalization to expression of P0. Primers used are as follows: P0 forward primer: 5′-GCGACCTGGAAGTCCAACT-3′, and P0 reverse primer: 5′-CCATCAGCACCACAGCCTTC-3′, sFRP-1 forward primer: 5′-AAGTCAGGGTGATTGGGGGAATCC-3′, and sFRP-1 reverse primer: 5′-AAACCATCTCCTCGGATAGGGCAC-3′, bov sFRP-1 forward 5′-ATTGAGCATCTCTGTGCCAGCGAG-3′, and bov sFRP-1 reverse primer: 5′-AAGACCGACTGGAAAGTGGGACAC-3′.

Generation of Transgenic Mice

Two types of transgenic mouse lines were generated. The first type of transgenic mouse line, Tie2 tTA mice,

express a tetracycline-controlled transactivator (tTA) under the control of mouse *Tie2* promoter/enhancer sequences. Several of the six independently raised lines exhibit doxycycline-regulatable transgene expression. Two to three-month-old mice from one of these lines (no. 7770) were used for this study. The second type of transgenic mouse line was produced by microinjection of a construct containing the bidirectional tet-responsive promoter, which allows the simultaneous expression of bovine sFRP-1 and β-galactosidase.[25] Two independent mouse lines (lines 11 and 56) were used for phenotypic analysis. Double-transgenic (Tie2-tTA/TRE-bov sFRP-1) mice were obtained by crossing the TRE-bov sFRP-1 mice with the *Tie2*-tTA transactivator mouse strain (Figure 7a). TRE-bov sFRP-1 and Tie2-tTA monotransgenic littermates were not different from wild-type mice (not shown) and TRE-bov sFRP-1 were used as controls. Because male and female mice exhibited the same phenotype, the data were pooled for controls as well as for double-transgenic mice.

For the genotyping, genomic DNA was isolated from mouse tail biopsies using the NucleoSpin tissue kit according to the manufacturer's instructions (Macherey-Nagel) and was analyzed by PCR. *Bov sFRP-1* and *tTA* transgenes were routinely detected, respectively, with the following primers: bov sFRP-1 forward primer: 5′-TGTGTCCTCCATGTGACAACGAGC-3′, and bov sFRP-1 reverse primer: 5′-TGAGATGAGTTTTTGTTCGGGC-3′, tTA forward primer: 5′-GCTGCTTAATGAGGTCGG-3′, and tTA reverse primer: 5′-CTCTGCACCTTGGTGATC-3′.

To assess whether transgene expression was confined to endothelial cells, experiments were performed on 11.5 dpc embryos (Figure 7b, see below) and on ischemic muscle from 10- to 12-week-old Tie2-tTA/TRE-bov sFRP-1 mice and single transgenic littermates (Figure 7d). β-Galactosidase expression was evaluated by histochemical staining with the chromogenic substrate X-Gal or by immunohistochemical staining using polyclonal antibody anti-β-galactosidase as previously described (Figure 7d, see below).[27]

Regulated Expression of the bov sFRP-1 Transgene in Tie2-tTA/TRE-bov sFRP-1 Mice

To repress tTA-dependent transactivation and bov sFRP-1 expression, doxycycline was given at 0.2 mg/ml in drinking water bottles containing 2.5% sucrose and wrapped with aluminum foil. The water containing doxycycline was changed every 2 days to avoid precipitation. Doxycycline was started 3 days before the surgery and maintained up to the time of sacrifice. Doxycycline inhibits matrix metalloproteinases,[28] which can be associated with alterations in vessel geometry. We found no adverse effects of doxycycline on vessel structure or growth when administered to mice for as long as 2 months. We verified that in littermates, doxycycline treatment had no significant effects on proliferation index or capillary density at any of the time points studied after ischemia (data not shown).

Mouse Model of Unilateral Hindlimb Ischemia

Unilateral hindlimb ischemia was operatively induced as previously described.[14] Exposure was obtained by performing an incision in the skin overlying the middle portion of the left hindlimb in each mouse. The proximal end of the femoral artery and the distal portion of the saphenous artery were both ligated, and the arteries as well as all side branches were excised. Ischemia was performed on binary Tie2-tTA/TRE-bov sFRP-1 or littermate mice with or without doxycycline. After the onset of ischemia, bovine sFRP-1 transcripts and X-Gal-positive cells were detected in many endothelial cells participating in the neovascularization of the ischemic muscle. This study was conducted in accordance with both institutional guidelines and those in force in the European community for experimental animal use (L358-86/609/EEC).

Modulation of Transgene Expression

To understand the specific effect of bov sFRP-1 overexpression in the late phase of neovascularization after ischemia, doxycycline was started 3 days before the surgery and maintained 6 days after. To induce expression of the transgene, doxycycline was withdrawn from the water and animals were killed at defined time points. Control animals were treated with doxycycline until sacrifice. Previous experiments have shown that sFRP-1 was expressed 2 days after doxycycline removal.

In ischemic muscle, bovine sFRP-1 mRNA expression was completely switched off after 6 or 21 days of doxycycline treatment in Tie2-tTA/TRE-bov sFRP-1 mice, thus indicating the conditional regulation of bovine sFRP-1. This regulation was further confirmed at the protein level by the lack of β-galactosidase-positive cells, as evidenced by X-Gal staining or labeling by the anti-β-galactosidase antibody (data not shown). These results demonstrate a tight suppression achieved by doxycycline on bovine sFRP-1 expression and the low probability of leaky bovine sFRP-1 transgene expression from tTA-mediated transactivation.

Necropsy Examination

Tissue Preparation

Animals were sacrificed at different time points with an overdose of sodium pentobarbital. For immunohistochemistry, anterior tibialis muscles were fixed in methanol and embedded in paraffin. For protein or RNA extraction, tissue samples were rinsed in PBS to remove excess blood, snap-frozen in liquid nitrogen, and stored at −80°C until used. A minimum of eight animals was examined for each time point in the littermate group and in the binary Tie2-tTA/TRE-bov sFRP-1 group.

Immunohistochemistry

Five-μm, paraffin-embedded sections cut transversely to the mouse muscle were used for immunohistochemis-

try. Commercially available antibodies were used to detect β-galactosidase (β gal; Chemicon) and endothelial cells (CD-31; Pharmingen). For measurement of capillary density, tissues were prepared as described.[14] Two different sections were taken from each part of the muscle. A minimum of 30 randomized pictures was recorded at ×40 magnification for each animal at each time point on the two sections with a camera connected to a PC. Positive cells were manually counted on captured images, and data were analyzed with Sigma Plot software. Capillary density was recorded as the number of capillaries per mm^2.

Statistical Analysis

Results are expressed as mean ± SD. All analyses were performed with appropriate software (Statview 5–1; Abacus). Comparison of continuous variables between two groups was performed by a one-way analysis of variance and subsequently, if statistical significance was observed, by a two-sided paired *t*-test. A value of $P < 0.05$ was considered significant.

Results

sFRP-1-Induced Endothelial Cell Spreading and Cytoskeletal Reorganization Is Matrix-Specific and Integrin-Dependent

Exposure to the recombinant bovine sFRP-1 (rb sFRP-1) protein enhanced the velocity of EC spreading on laminin and type I and IV collagen (130 ± 9%, 127 ± 18%, and 127 ± 14%, respectively, at 2 hours) (Figure 1a). Interestingly, sFRP-1 failed to induce cell spreading on polylysine, to which cells attach by charge interactions alone suggesting that sFRP-1 influences EC spreading in a matrix-dependent manner. Similar results were observed with PAECs (data not shown).

More strikingly, the surface area of ECs under rb sFRP-1 treatment increased as compared to control conditions (1.9-fold increase) (Figure 1a). This increase in large, flattened cells under rb sFRP-1 stimulation was correlated with a rearrangement of the actin cytoskeleton. rb sFRP-1 treatment of ECs stimulated the formation of actin stress fibers and focal contacts that were detectable, respectively, with phalloidin and vinculin staining (Figure 1b).

As interaction between vinculin and actin filaments is thought to constitute an interface between the cytoskeleton and the integrins,[29] we next sought to investigate the involvement of integrin in sFRP-1-induced EC spreading. Although addition of blocking antibody (Ab) for β1- or α2β1-integrin, completely blocked the sFRP-1-induced HUVEC spreading on both collagen type I (Figure 1c) and laminin (not shown), a function-blocking Ab directed against αvβ3-integrin (LM609) did not affect sFRP-1-induced EC spreading on both matrices. These results were confirmed in PAECs (data not shown). Integrin activation by rb sFRP-1 was showed via a rapid induction of phospho-α-PAK (Supplementary Figure 1, see *http://ajp.amjpathol.org*) in HUVECs. Using FACS analysis, we demonstrated that β1-integrin levels were not modulated on the surface of sFRP-1-treated HUVECs and PAECs, compared to control levels at 4 and 16 hours after cell activation (Supplementary Figure 2, see *http://ajp.amjpathol.org*). sFRP-1 may participate in an inside-outside signaling process that promotes α2β1-integrin affinity. These data suggest a cooperative effect of sFRP-1 and integrin pathways in ECs.

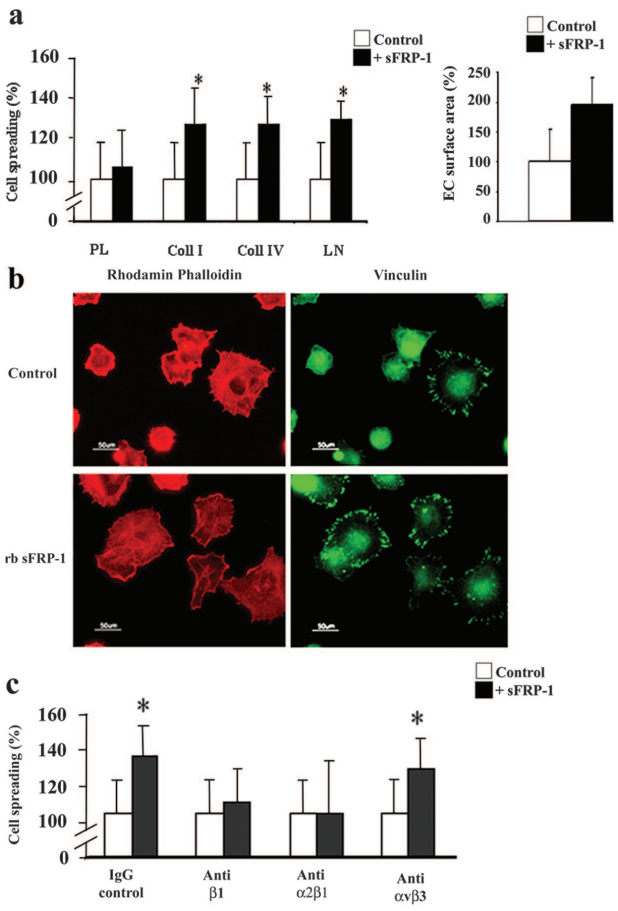

Figure 1. sFRP-1 induces HUVEC spreading on extracellular matrix and promotes HUVEC cell spreading to collagen type I through α2β1-integrin. **a:** HUVECs were allowed to spread on polylysine (PL), type I collagen (Coll I), type IV collagen (Coll IV), or laminin (LM) in the absence or presence of rb sFRP-1 in serum-free medium for 2 hours. The percentage of spread cells were scored as described in the Materials and Methods section. Cell surface area was quantified in adherent HUVECs after staining by rhodamine-phalloidin Treatments were performed in triplicate, and results are expressed as mean percent spreading ± SD. *$P < 0.05$ relative to controls. **b:** F-actin (red fluorescence) and focal adhesion plaque (green fluorescence) distributions were detected in adherent HUVECs after staining with rhodamine-phalloidin or vinculin labeling in the absence (control) (□) or in the presence (■) of recombinant bovine sFRP-1 (+rb sFRP-1). **c:** Spreading assays of HUVECs were performed in the presence of function-blocking antibodies against β1, α2β1, and αvβ3 integrins on wells coated with type I collagen. A mouse IgG served as control. Cells were preincubated for 15 minutes before plating with function-blocking mAbs at a concentration of 4 μg/ml in the absence (□) or presence (■) of recombinant bovine sFRP-1. Spreading was quantified by counting the number of spread cells per field as described in the Materials and Methods section (×20 objective). Results are expressed as mean spreading as percentage of control ± SD. *$P < 0.05$ relative to controls.

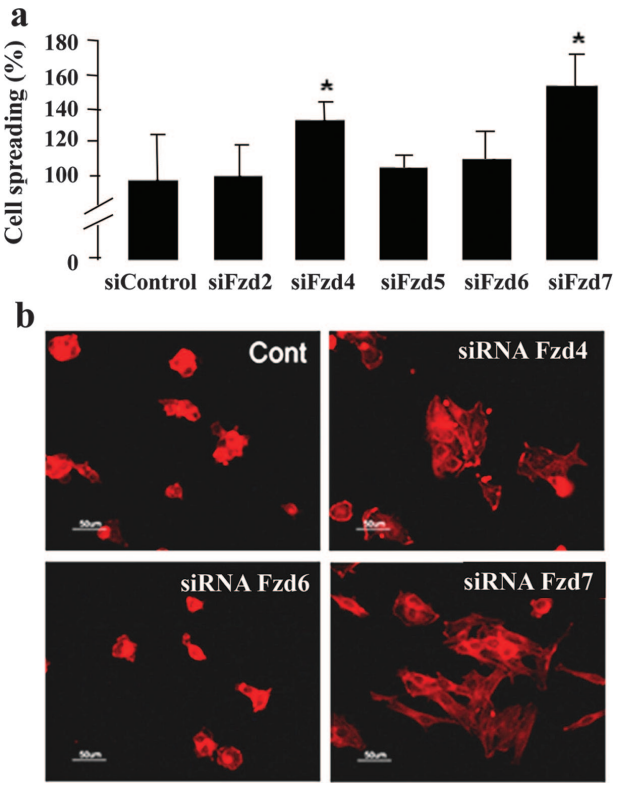

Figure 2. Involvement of Frizzled 4 and 7 in sFRP-1-induced endothelial cell spreading. Forty-eight hours after transfection with siRNA control or indicated Frizzled siRNA (Fzd2, Fzd4, Fzd5, Fzd6, Fzd7), MS1 cells were submitted to a spreading assay on wells coated with type I collagen. **a:** The percentage of spread cells were scored as described in the Materials and Methods section. **b:** F-actin (red fluorescence) distribution in adherent MS1 cells was detected by rhodamine-phalloidin.

Frizzled 4 and 7 Receptors Are Involved in EC Spreading

We then addressed whether EC spreading involved Fzd receptor blockade. Murine EC line MS1 expressed *Fzd2*, *4*, *5*, *6*, and *7* transcripts and a very low level of *Fzd1* transcripts. Noteworthy, the same expression profile was found in HUVECs (Supplementary Figure 1a, see *http://ajp.amjpathol.org*).[30] We used siRNA targeted to *Fzd2*, *4*, *5*, *6*, and *7* and showed by RT-PCR that RNA interference assays efficiently decreased the mRNA levels of the distinct Fzd genes (from ~60 to 95% efficiency) (Supplementary Figure 3b, see *http://ajp.amjpathol.org*). siRNA targeting one specific member of the Fzd family did not inhibit the expression of other Fzd members in MS1 cells (data not shown), suggesting a highly specific siRNA effect.

Treatment with control or Fzd2, -5, and -6 siRNA did not modulate EC spreading. In contrast, Fzd4 or -7 depletions dramatically increased EC spreading (136 ± 16% and 147 ± 9%, respectively) (Figure 2a) and induced large and abundant flattened ECs as observed after F-actin staining (Figure 2b). These experiments revealed a direct involvement of Fzd4 and Fzd7 in spreading. These results were confirmed on HUVECs (data not shown).

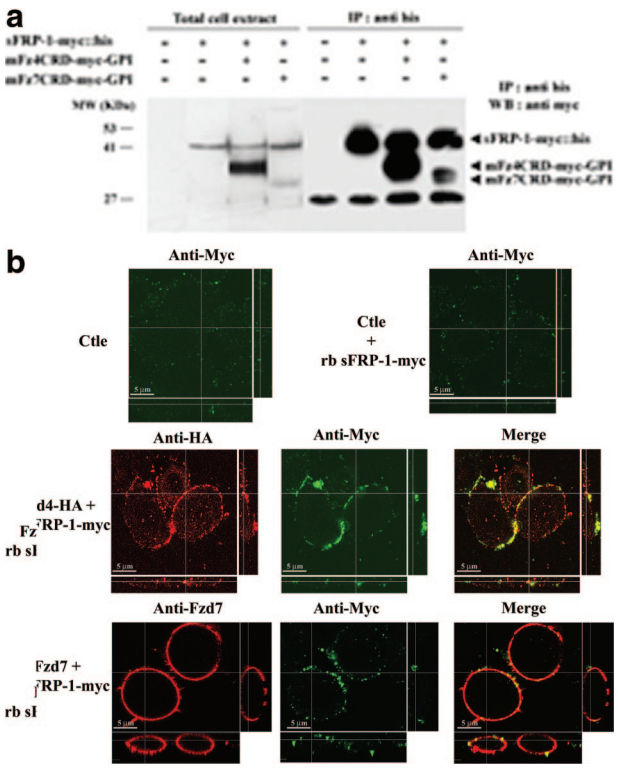

Figure 3. Interaction between sFRP-1 and extracellular domain of Frizzled 4 and Frizzled 7 *in vitro*. **a:** CHO cells were transfected with expression vectors as indicated. Total cell extract (T) were immunoprecipitated (IP) with anti-His tag antibody. The immunoprecipitates were immunoblotted (WB) with anti-myc tag antibody. Positions of specific bands corresponding to bovine sFRP-1-myc::his, mFz4CRD-myc-GPI, or mFz7CRD-myc-GPI are indicated. **b:** CHO cells expressing either Fzd4-HA or Fzd7 or none (Ctle) were incubated with rb sFRP-1-myc for 1 hour. Fzd4 and Fzd7 expressed, as determined by using histochemical detection (red staining), localized efficiently at the cell membrane, and induced accumulation of sFRP-1 puncta (green). This recruitment and co-localization of Fzd4 or Fzd7 with sFRP-1 in puncta could highlight sites of frizzled activity.

sFRP-1 Interacts with Frizzled 4 and 7 Receptors

sFRP-1-treated cells or Fzd4 and Fzd7 knockdown cells presented a similar behavior during spreading assays compared to that of control cells. We thus explored whether sFRP-1 interacts directly with Fzd4 and -7. Addition of rb sFRP-1 to mFzd4CRD-myc-GPI-expressing CHO cells resulted in efficient co-precipitation of mFzd4 protein with the his-tagged sFRP-1. Precipitation of rb sFRP-1 in CHO cells transfected with mFzd7CRD-myc-GPI showed a minor co-precipitation of mFzd7 protein (Figure 3a). To determine the localization of rb sFRP-1 on CHO overexpressing Fzd4 and Fzd7, by confocal microscopy analysis, CHO, transfected with plasmids harboring Fzd4-HA and Fzd7, were incubated with the recombinant protein rb sFRP-1-myc. In the absence of Fzd overexpression (ctle), rb sFRP-1 was poorly detected in CHO in a few plasma membrane puncta (Figure 3b). Transfection of plasmid harboring Fzd4-HA and Fzd7 showed a strong expression and localization of each Fzd at the cell membrane as revealed by a red staining. In the presence of full-length Fzd4 and -7 in CHO, rb sFRP-1 was found in

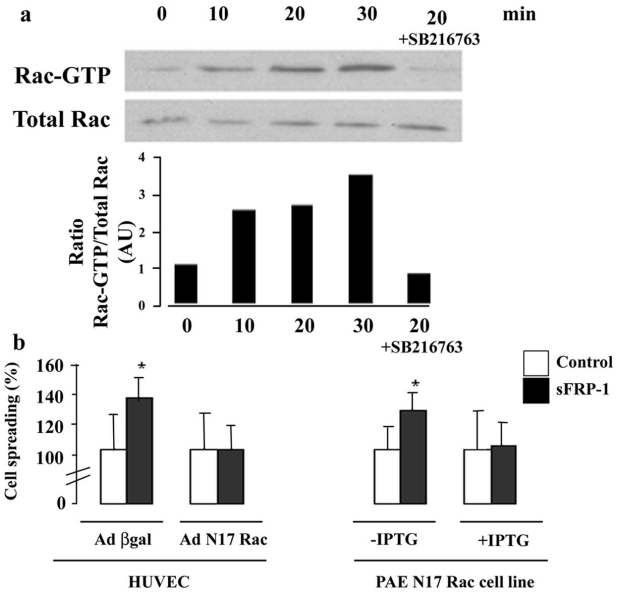

Figure 4. Role of Rac1 in sFRP-1 induced spreading on endothelial cells. sFRP-1 leads to an activation of Rac1, which is required for sFRP-1-induced EC spreading. **a:** Immunoprecipitation using a GST-human PAK1-PBD fusion protein that binds to GTP-bound Rac1 (active form) was used to detect, by Western blotting, the magnitude of Rac1 activation in response to sFRP-1 in HUVECs. Serum-starved HUVECs were exposed or not to recombinant bovine sFRP-1 for the indicated times. Cells were also pretreated with SB 216763 (10 μmol/L) before stimulation. The results are expressed as Rac GTP/total Rac ratio and are representative of three independent experiments. **b:** HUVECs were infected with adenovirus expressing the β-galactosidase or the dominant-negative form of Rac1 (Ad N17Rac) 18 hours before stimulation with the recombinant bovine sFRP-1. The PAE cell line expressing N17 Rac under the control of an IPTG-inducible promoter was also treated by recombinant bovine sFRP-1. After stimulation, spreading assays on type I collagen were performed as described in the Materials and Methods section. Data are expressed in average percent spreading ± SD ($n = 3$). *$P < 0.05$ relative to control without recombinant bovine sFRP-1.

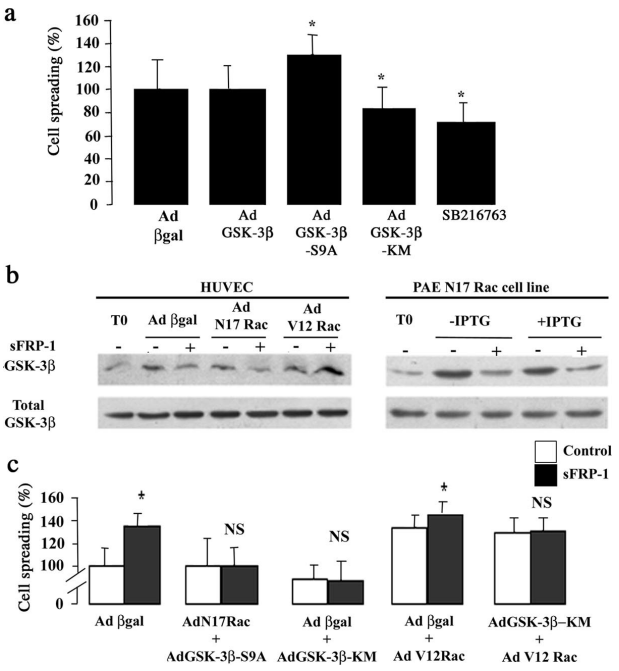

Figure 5. GSK-3β/Rac-1 pathway involved in sFRP-1-induced EC spreading. **a:** HUVECs were either infected with adenovirus expressing β-galactosidase, GSK-3β, GSK-3β-S9A, or GSK-3β-KM or treated with SB216763. After the treatment, a spreading assay was performed. Data are mean percent spreading ± SD. *$P < 0.05$ relative to control. **b:** HUVECs infected with adenovirus coding for β-galactosidase or N17Rac or V12Rac and PAE cell line expressing N17Rac under the control of an IPTG-inducible promoter were also treated or not with recombinant bovine sFRP-1 for 30 minutes in serum-free medium. After stimulation, the cellular proteins were analyzed by Western blotting with anti-phospho-GSK-3β (Ser 9) and total GSK-3β. The results shown are representative of three independent experiments. **c:** HUVECs were infected in a two-step process: first with adenovirus coding for β-galactosidase, N17Rac, or GSK-3β-KM, 6 hours before a second infection with adenovirus producing β-galactosidase, GSK-3β-S9A, GSK-3β-KM, or V12Rac. Eighteen hours later, cells were treated (■) or not (□) with rb sFRP-1 for 30 minutes in serum-free medium. After stimulation, spreading assays on type I collagen were performed as described in the Materials and Methods section. Data are mean percent spreading ± SD. *$P < 0.05$ relative to control without recombinant bovine sFRP-1.

regions that co-localized with Fzd4-HA and -7 accumulations as revealed by a yellow coloration (Figure 3b). These rb sFRP-1 accumulations were larger and more uniformly to the plasma membrane in Fzd4-HA-transfected CHO than in Fzd7-transfected CHO confirming our previous observation showing that sFRP-1 binds more efficiently to Fzd4 than to Fzd7. Altogether, these data demonstrate that sFRP-1 interacts with both Fzd receptors and suggest that sFRP-1 is an antagonist of both Fzd4 and Fzd7 receptors.

sFRP-1-Induced EC Spreading Involves Rac1 Activation

The process of cell spreading involves control of the complex dynamic rearrangements of the actin cytoskeleton by members of the Rho GTPase family such as Rac1.[31,32] Because sFRP-1 modifies cytoskeleton organization, we investigated whether Rac1 could be an effector of sFRP-1 pathway. Pull down assays showed a rapid activation of Rac1 (GTP-Rac) in HUVECs after 10 to 30 minutes of rb sFRP-1 treatments (Figure 4a). Similar results were observed for PAECs (data not shown). The Rac1 dominant-negative mutant adenovirus (AdN17Rac) abolished sFRP-1 effects on HUVEC spreading whereas control adenoviral vector (Ad βgal) did not modify EC response to rb sFRP-1 (Figure 4b). Similar results were observed in a PAE cell line in which overexpression of N17Rac is under the control of an IPTG-inducible promoter (Figure 4b). The activation of Rac1 by sFRP-1 appeared to be critical for EC spreading enhancement.

EC Spreading Requires Cooperative Activation of GSK-3β and Rac1

Our previous observations and preliminary experiments indicating that rb sFRP-1 abrogated GSK-3β inactivation by preventing its phosphorylation at Ser9 residue[15]prompted us to examine the involvement of GSK-3β in EC spreading. HUVECs were thus either transduced with adenoviruses harboring a wild-type (Ad GSK-3β-WT), a constitutively active, unphosphorylatable form (GSK-3β-S9A), or a dominant-negative form (Ad GSK-3β-KM) of GSK-3β or treated with a selective GSK-3β inhibitor, SB216763. GSK-3β-WT overexpression had no effect on EC spreading (Figure 5a). GSK-3β-S9A overexpression caused a 30% increase in EC spreading (130 ± 17% compared to

control Ad βgal adenovirus). Both AdGSK-3β-KM delivery and the pharmacological inhibitor of GSK-3β decreased the HUVEC's basal spreading level, ie, 83 ± 18% and 71 ± 17%, respectively, compared with control (Figure 5a). The same results were obtained on PAECs (data not shown). These findings suggest a role for GSK-3β activation in regulation of EC spreading.

We hypothesized that GSK-3β and Rac1 could act, in the same pathway, on sFRP-1-mediated EC spreading. We first showed that inhibition of GSK-3β completely blocked rb sFRP-1-induced EC spreading on type I collagen (Figure 5c). Treatment of cells with the SB216763 inhibitor of GSK-3β blocked the ability of rb sFRP-1 to activate Rac1 (Figure 4a). Second, we demonstrated that the overexpression of the dominant-negative form of Rac1 (N17Rac) in ECs, either by HUVEC adenovirus (AdN17Rac) infection or by IPTG induction in PAE N17 Rac-inducible cell line, did not affect the level of GSK-3β phosphorylation by sFRP-1 (Figure 5b). All these data suggest that GSK-3β was able to act upstream of Rac 1 under sFRP-1 treatment. These results were confirmed when co-expression of N17Rac and GSK-3β-S9A adenoviruses failed to restore EC spreading in response to rb sFRP-1, demonstrating that GSK-3β acts upstream of Rac1 in sFRP-1-induced EC spreading (Figure 5c).

AdV12Rac expression resulted in a significant increase of EC spreading compared with Ad βgal-infected ECs, ie, 133 ± 13% of control, indicating an effect of Rac1 itself on EC spreading (Figure 5c). Moreover, we found an additive effect of sFRP-1 on V12Rac-expressing EC spreading ie, 146 ± 11% of control (Figure 5c). Taken together, these experiments place Rac1 under GSK-3β activation in the sFRP-1-dependent signaling cascade that leads to EC spreading.

EC Spreading Is Independent of the Activation of the Wnt Canonical Pathway and Depends on a GSK-3β Pathway

sFRP-1 is usually considered as a Wnt canonical pathway antagonist. Here, we sought to determine whether sFRP-1 effect on EC spreading was dependent on activation of the Wnt canonical pathway using a β-catenin-deleted EC line.[33] Depletion of β-catenin did not affect sFRP-1 spreading enhancement (Figure 6a), although dominant-negative overexpression of GSK-3β blocked sFRP-1-induced spreading. These results confirm that the antagonistic function of sFRP-1 is independent of the canonical Wnt pathway but involves GSK-3β activation.

Correlation of an sFRP-1/GSK-3β-Dependent Pathway Activation with Vascular Formation

We further sought to test whether induction of the GSK-3β/Rac-1 pathway plays a role on EC organization during neovessel formation. We took advantage of an inducible approach based on the tTA system[34] combined with the Tie2 endothelial cell-specific promoter[35,36] to regulate

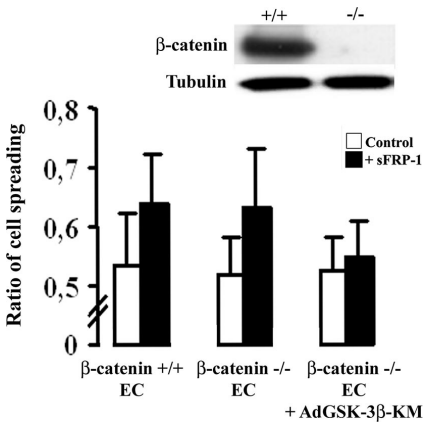

Figure 6. sFRP-1 induction of EC spreading is independent of β-catenin and requires GSK-3β activation. Endothelial cell lines expressing β-catenin (+/+) or deleted for β-catenin (−/−) as demonstrated by Western blot, were treated (■) or not (□) with rb sFRP-1 for 30 minutes in serum-free medium. The role of GSK-3β was investigated in ECs deleted for β-catenin by infection of ECs with adenovirus expressing GSK-3β-KM. After stimulation, spreading assays on type I collagen were performed as described in the Materials and Methods section. Data are mean percent spreading ± SD. $^*P < 0.05$ relative to control without recombinant bovine sFRP-1.

bovine transgene sFRP-1 expression specifically in the EC during vessel formation (Figure 7a).

We used inducible Tetoff transgenic mice, in which expression of the transgene, bov sFRP-1, was repressed by doxycycline treatment when added to the drinking water. During pregnancy, the females were never under doxycycline treatment. The transgene was not repressed during embryonic development, and we did not observe any obvious alteration during embryonic vascular development in double-transgenic embryos (Tie2-tTA/TRE-bov sFRP-1) (Figure 7b).

When we overexpressed bov sFRP-1 transgene all along the kinetics of repair in the Tie2-tTA/TRE-bov sFRP-1 double-transgenic mice, we observed a delay in capillary formation until day 14 after the surgery, ie, 495.5 ± 272.2 capillaries/mm^2 for Tie2-tTA/TRE-bov sFRP-1 versus 782.,1 ± 238.5 for littermates, at day 15, $P < 0.001$. After 14 days, capillary number had further increased in Tie2-tTA/TRE-bov sFRP-1 ischemic muscle. At day 25, capillary density in the Tie2-tTA/TRE-bov sFRP-1 mice ischemic hindlimbs was significantly higher than in those of littermates, ie, 1416 ± 74 capillaries/mm^2 for Tie2-tTA/TRE-bov sFRP-1 versus 1092 ± 59 for littermates, $P < 0.005$ (Supplementary Figure 4, see *http://ajp.amjpathol.org*).

Because sFRP-1 has been described as being expressed long after muscle ischemia,[37] and because it alters cell cycle in vascular cells,[14] we decided to overexpress sFRP-1, not in the precocious phase of muscle repair but 7 days after injury in a model of hindlimb ischemia. In the mouse model of hindlimb ischemia, we showed by qRT-PCR that endogenous sFRP-1 expression was regulated during muscle repair: a strong but late induction of sFRP-1 was observed with a peak at day 7 after injury. At day 14, sFRP-1 expression declined and then returned to near basal level at day 25 (Supplementary Figure 5, see *http://ajp.amjpathol.org*).

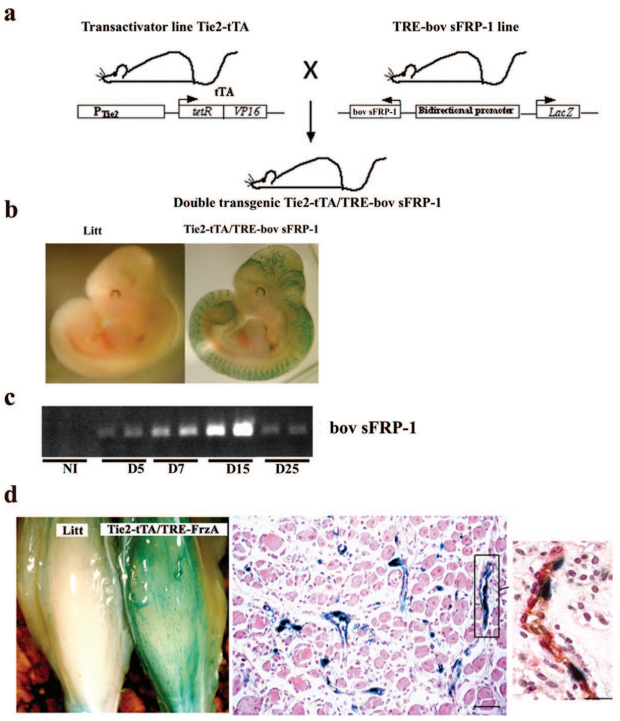

Figure 7. Characterization of the Tie2-tTA/TRE-bov sFRP-1 mice. **a:** Tie2-tTA transactivator mouse line expressing tTA under the control of the endothelial-specific *tie2* promoter was mated with TRE-bov sFRP-1 transgenic mice leading to double-transgenic mice with inducible and endothelium-restricted expression of bovine sFRP-1 and of *LacZ* as reporter gene. **b:** LacZ transgene expression was confined to endothelial cells in Tie2-tTA/TRE-bov sFRP-1 compared to littermate embryo (Litt) at day 11.5 dpc. β-galactosidase expression was evaluated by staining with the chromogenic substrate X-Gal on paraformaldehyde 2% fixed embryos *in toto*. **c:** Expression by RT-PCR of bov sFRP-1 during the kinetics of ischemia. **d:** LacZ transgene expression in Tie2-tTA/TRE-bov sFRP-1 in hindlimb after ischemia: at day 11 after ischemia. X-Gal staining of whole mount hindlimb of Litt and Tie2-tTA/TRE-bov sFRP-1 mice and of thin section displayed strong expression of LacZ in neovessels. Section and **inset** was X-Gal stained for lacZ expression and then double-immunostained with anti-CD31 (in brown) and anti-α-actin (in red) antibodies to localize blood vessel endothelium and pericytes at day 11 in Tie2-tTA/TRE-bov sFRP-1 mice. X-Gal staining demonstrated the selective expression in ECs of neovessels. Scale bar = 50 μm.

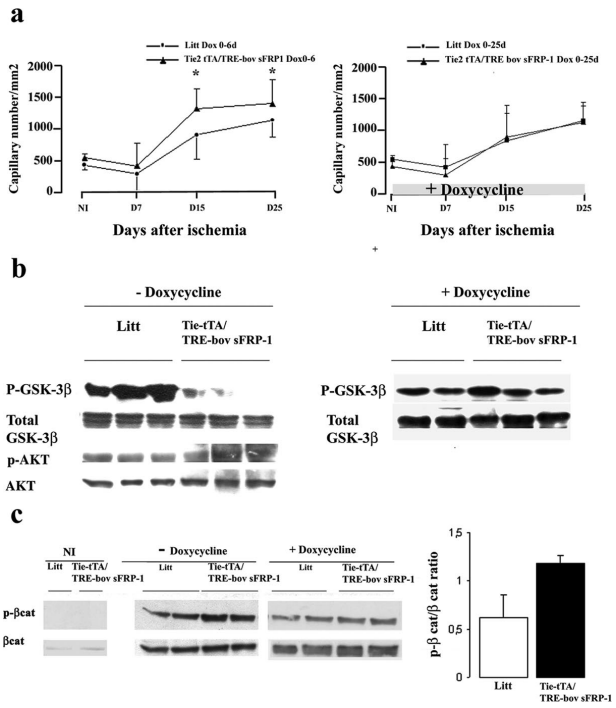

Figure 8. Role of sFRP-1 in neovessel formation and on the level of phosphorylated GSK-3β and β-catenin after hindlimb ischemia. **a:** Quantitative evaluation of capillary density using CD31 immunostaining (number of vessels/mm^2) in tissues retrieved from ischemic anterior tibialis muscle of littermates and Tie2-tTA/TRE-bov sFRP-1 mice treated from day 0 to day 6 with doxycycline (Dox, 0 to 6 days) after ischemia. $^*P < 0.001$ and in mice treated with doxycycline after ischemia, from day 0 to day 25 (Dox, 0 to 25 days) after ischemia with doxycycline. $^*P < 0.001$. Treatment through the whole period of ischemia with doxycycline in Tie2-tTA/TRE-bov sFRP-1 animals, switched off bovine sFRP-1 expression and restored a kinetics of capillary density similar to that in littermates, thereby confirming the specific role of endothelial bovine sFRP-1 in the modulation of the angiogenic response after ischemia. The levels of either p-GSK-3β and GSK-3β total (**b**) or p-β-catenin and total β-catenin (**c**) was compared by Western blot in Tie2-tTA/TRE-bov sFRP-1 versus littermate (Litt) in hindlimb extracts at day 15 after ischemia. Doxycycline was removed from the drinking water 6 days after ischemia, allowing sFRP-1 induction (−doxycycline). Controls were done with mice treated from day 0 to day 15 after injury with doxycycline (+doxycycline). A quantification of the ratio of phospho-β-catenin:β-catenin is presented.

Here, we repressed sFRP-1 expression from day 0 to day 6 after ischemia with doxycycline treatment (OFF). Then doxycycline was withdrawn from the drinking water to allow re-expression of the transgene (ON). The activation of the transgene expression after 7 days of ischemia resulted in a very large increase in capillary density at 15 days in transgenic mice compared to littermates and maintained at day 25, ie, 1318 ± 318 capillaries/mm^2 for Tie2-tTA/TRE-bov sFRP-1 versus 907 ± 382 capillaries/mm^2 for littermates, $P < 0.005$ at day 15; and 1406 ± 366 capillaries/mm^2 for Tie2-tTA/TRE-bov sFRP-1 versus 1141 ± 261 capillaries/mm^2 for littermates, $P < 0.005$ at day 25 (Figure 8a). This effect on vessel formation was abolished in transgenic animals treated with doxycycline (Figure 8a).

sFRP-1 overexpression induced a dramatic decrease in Ser9 phospho-GSK-3β levels in double-transgenic hindlimb extracts in comparison to those in littermate extracts at 15 days (Figure 8b). The decrease in phospho-GSK-3β levels was not found when Tie2-tTA/TRE-bov sFRP-1 mice were treated with doxycycline. Total GSK-3β levels were unchanged before and after ischemia (not shown) and between the two mouse groups at 15 days after ischemia (Figure 8b).

In parallel, we monitored β-catenin and phospho-β-catenin levels in the cytosolic fractions of hindlimb extracts as markers of the canonical Wnt-frizzled pathway. At 15 days after surgery, total cytosolic β-catenin was increased in ischemic hindlimb tissues compared to that in nonischemic tissues. The pattern of total cytosolic β-catenin expression was comparable in Tie2-tTA/TRE-bov sFRP-1 and littermate hindlimb extracts. Phospho-β-catenin was slightly increased in binary transgenic animals at day 15 (Figure 8c). This effect was reversed in double-transgenic animals treated with doxycycline (Figure 8c).

Discussion

It has been recently put forward that the Wnt pathway is involved in vessel formation although its contribution has

been essentially demonstrated through gene inactivation models.[8,9,10,11] The secreted factor sFRP-1 is able to bind both Wnt proteins and Fzd receptors.[7] It has been used as a modulator of the Wnt-β-catenin pathway, to study Wnt involvement in vessel biology.[38] We have previously demonstrated that *in vitro* sFRP-1 modulated EC angiogenic response (migration, differentiation) and *in vivo* stimulated neovascularization in plug or tumor models.[15] These angiogenic effects seemed independent of the vascular endothelial growth factor pathway. Our present study has unraveled new molecular players in the Wnt/Fzd complex cascade regulating EC behavior during *de novo* vessel formation.

Directed movements of EC during *de novo* vessel formation are coordinated through cellular adhesion mechanisms, cytoskeletal reorganization, and in association with elevated expression of angiogenic factors such as the key factor vascular endothelial growth factor. The regulation of EC cytoskeleton is essential to EC spreading and motility.[29] We demonstrate that sFRP-1 had a major role in mediating EC spreading by regulating reorganization of the actin network and focal contact formations. We demonstrated that sFRP-1-induced spreading was extracellular matrix-dependent and involved $\alpha 2\beta 1$ integrin activation. Several publications have recently demonstrated the role of the Wnt/Fzd pathway in cell cytoskeletal remodeling.[39,40] Interaction between Dishevelled, a common central Wnt mediator, and Rac1 is involved in dendrite morphogenesis through Wnt7b.[39] Interference with Dishevelled 2 expression disorganized the actin cytoskeleton in ECs, altering their capacities to form lamellipodia.[40] Because, the family of the Rho GTPase is important in various aspects of EC cytoskeletal organization, we predicted the participation of Rac1 in sFRP-1-induced spreading. We demonstrated that Rac1 acts downstream of GSK-3β in the sFRP-1 signaling pathway inducing EC spreading. As Rho GTPase regulated the actin cytoskeleton, our results suggest that sFRP-1, through the activation of GSK-3β and Rac1, modulates EC organization by regulating the dynamics of actin.

sFRP-1 is a proposed Wnt/Fzd signaling inhibitor, but recent reports showed that sFRP could act through Wnt-independent mechanisms.[41–43] In our study, the effect of sFRP-1 on EC spreading is independent of the canonical β-catenin pathway *in vitro* (Figure 2a) but involves GSK-3β machinery. sFRP-1 has been shown to be able to modulate retinal cell differentiation via the phosphorylation on the Ser9 residue of GSK-3β.[44] Moreover, the existence of a noncanonical Wnt pathway involving GSK-3β has been proposed to regulate cell movement and differentiation, whereas enhanced expression of Wnt2 has been associated with tumoral proinvasive activity and coupled to GSK-3β inhibition.[45] However, our results contrast with the study of Kim and colleagues[46] analyzing the effect of GSK-3β on EC properties and angiogenesis and reporting inactivation of GSK-3β as a key regulator of angiogenesis after ischemia. In their study, inactivation of GSK-3β was induced by phosphorylation via upstream PKB/AKT or protein kinase C activation. In our *in vivo* model or in cultured ECs, the sFRP-1-induced decrease of GSK-3β phosphorylation state was independent of any modification of PKB/AKT phosphorylation (Figures 5b and 8b).[15] Although the reason for this discrepancy is unknown, it may indicate differences in GSK-3β upstream modulation and the influence of Wnt signaling in EC behavior. Based on our observations, we propose that the regulation of GSK-3 β activity via sFRP-1, promotes EC spreading and morphological organization.

It has been recently suggested that sFRP-1 plays the role of a morphogen that could govern the growth of retinal ganglion cell axons. This activity seemed independent of Wnt inhibition but attributable to a direct interaction with an Fzd receptor Fzd2.[47] We and others[30] have reported that ECs were equipped with distinct Frizzled receptors, which led us to evaluate the possible involvement of the Fzd receptors in EC spreading. We demonstrated that sFRP-1 interacted and co-localized with Fzd4 and Fzd7. The functions of some Fzd receptors have recently been explored in mammals. Examination of mice deleted for Fzd4 receptor demonstrated the crucial role of *Fzd4* in the migration of ECs along the retinal surface.[9] *Fzd7* has been shown to be involved in neural crest migration.[48] Using an siRNA-based strategy, inhibition of Fzd4 and Fzd7 expression enhanced EC spreading, inducing large and flattened cells mimicking the EC spreading effect of sFPR-1. It is therefore tempting to speculate that sFRP-1 could act through a dominant-negative mechanism interacting with the Fzd4 and 7 receptors forming nonfunctional complexes.

Our *in vivo* data support a critical role for sFRP-1 in ischemia-induced angiogenesis in adults. We have previously shown that impairment of the canonical Wnt/Fzd pathway in the early phase of ischemia using adenovirus-expressing sFRP-1 reduced vascular cell proliferation and delayed vessel formation.[14] Here, we set up an inducible system to overexpress the sFRP-1 transgene specifically in ECs using a *Tie2* promoter. When sFRP-1 was induced specifically in ECs all along the kinetics of ischemia repair, we obtained a biphasic response: a delay in capillary formation until day 15 and then an increase in vascular formation at day 25. The inducible system allowed a sequential expression of the transgene: ectopic sFRP-1 was repressed until day 6 with doxycycline treatment (OFF) and then induced at day 7 until day 25 by removing doxycycline (ON). Using this strategy, late ectopic expression of sFRP-1 augmented capillary formation and was correlated with GSK-3β activation. We observed a faint effect of bov sFRP-1 on phospho-β-catenin level induced by ischemia. The specificity of all of the effects was strengthened by the use of doxycycline as an internal control able to turn off sFRP-1 overexpression after injury.

This inducible transgenic model reveals that sFRP-1 could fine tune the outcome of Wnt/Fzd signaling at different steps in the course of neovessel formation. We propose a model in which sFRP-1 could regulate two processes. In the early angiogenic phases, sFRP-1 could regulate a canonical Wnt/Fzd signaling pathway to alter vascular cell proliferation and recent findings show that its effect is relayed by another pathway that could signal by activating GSK-3β and participate in neovessel orga-

nization. In conclusion, our study suggests that sFRP-1 might participate in postnatal neovascularization after an ischemic event through a GSK-3β/Rac1 pathway by blocking Fzd receptor in ECs.

Acknowledgments

We thank Dr. Jeremy Nathans for helpful comments on the manuscript and Dr. E. Dejana for providing β-catenin-deleted EC line, undertaken in the context of The European Vascular Genomics Network.

References

1. Cadigan KM, Nusse R: Wnt signaling: a common theme in animal development. Genes Dev 1997, 11:3286–3305
2. Huelsken J, Behrens J: The Wnt signalling pathway. J Cell Sci 2002, 115:3977–398
3. Pinson KI, Brennan J, Monkley S, Avery BJ, Skarnes WC: An LD L-receptor-related protein mediates Wnt signalling in mice. Nature 2000, 407:535–538
4. Logan CY, Nusse R: The Wnt signaling pathway in development and disease. Annu Rev Cell Dev Biol 2004, 20:781–810
5. Kuhl M: The WNT/calcium pathway: biochemical mediators, tools and future requirements. Front Biosci 2004, 9:967–974
6. Kawano Y, Kypta R: Secreted antagonists of the Wnt signalling pathway. J Cell Sci 2003, 116:2627–2634
7. Bafico A, Gazit A, Pramila T, Finch PW, Yaniv A, Aaronson SA: Interaction of frizzled related protein (FRP) with Wnt ligands and the frizzled receptor suggests alternative mechanisms for FRP inhibition of Wnt signaling. J Biol Chem 1999, 274:16180–16187
8. Ishikawa T, Tamai Y, Zorn AM, Yoshida H, Seldin MF, Nishikawa S, Taketo MM: Mouse Wnt receptor gene Fzd5 is essential for yolk sac and placental angiogenesis. Development 2001, 128:25–33
9. Xu Q, Wang Y, Dabdoub A, Smallwood PM, Williams J, Woods C, Kelley MW, Jiang L, Tasman W, Zhang K, Nathans J: Vascular development in the retina and inner ear: control by Norrin and Frizzled-4, a high-affinity ligand-receptor pair. Cell 2004, 116:883–895
10. Monkley SJ, Delaney SJ, Pennisi DJ, Christiansen JH, Wainwright BJ: Targeted disruption of the Wnt2 gene results in placentation defects. Development 1996, 122:3343–3353
11. Shu W, Jiang YQ, Lu MM, Morrisey EE: Wnt7b regulates mesenchymal proliferation and vascular development in the lung. Development 2002, 129:4831–4842
12. Blankesteijn WM, van Gijn ME, Essers-Janssen YP, Daemen MJ, Smits JF: Beta-catenin, an inducer of uncontrolled cell proliferation and migration in malignancies, is localized in the cytoplasm of vascular endothelium during neovascularization after myocardial infarction. Am J Pathol 2000, 157:877–883
13. Barandon L, Couffinhal T, Ezan J, Dufourcq P, Costet P, Alzieu P, Leroux L, Moreau C, Dare D, Duplaa C: Reduction of infarct size and prevention of cardiac rupture in transgenic mice overexpressing FrzA. Circulation 2003, 108:2282–2289
14. Ezan J, Leroux L, Barandon L, Dufourcq P, Jaspard B, Moreau C, Allieres C, Daret D, Couffinhal T, Duplaa C: FrzA/sFRP-1, a secreted antagonist of the Wnt-Frizzled pathway, controls vascular cell proliferation in vitro and in vivo. Cardiovasc Res 2004, 63:731–738
15. Dufourcq P, Couffinhal T, Ezan J, Barandon L, Moreau M, Daret D, Duplàa C: FrzA, a secreted Frizzled related protein, induced angiogenic response. Circulation 2002, 106:3097–3103
16. Arbiser JL, Moses MA, Fernandez CA, Ghiso N, Cao Y, Klauber N, Frank D, Brownlee M, Flynn E, Parangi S, Byers HR, Folkman J: Oncogenic H-ras stimulates tumor angiogenesis by two distinct pathways. Proc Natl Acad Sci USA 1997, 94:861–866
17. Davis W, Stephens LR, Hawkins PT, Saklatvala J: Synergistic activation of JNK/SAPK by interleukin-1 and platelet-derived growth factor is independent of Rac and Cdc42. Biochem J 1999, 338:387–392
18. Duplaa C, Jaspard B, Moreau C, D'Amore PA: Identification and cloning of a secreted protein related to the cysteine-rich domain of frizzled. Evidence for a role in endothelial cell growth control. Circ Res 1999, 84:1433–1445
19. Jaspard B, Couffinhal T, Dufourcq P, Moreau C, Duplaa C: Expression pattern of mouse sFRP-1 and mWnt-8 gene during heart morphogenesis. Mech Dev 2000, 90:263–267
20. Dufourcq P, Couffinhal T, Alzieu P, Daret D, Duplàa C, Bonnet J: Vitronectin is up regulated after vascular injury and vitronectin blockade prevents neointima formation. Cardiovasc Res 2002, 53:952–962
21. Coghlan MP, Culbert AA, Cross DA, Corcoran SL, Yates JW, Pearce NJ, Rausch OL, Murphy GJ, Carter PS, Roxbee Cox L, Mills D, Brown MJ, Haigh D, Ward RW, Smith DG, Murray KJ, Reith AD, Holder JC: Selective small molecule inhibitors of glycogen synthase kinase-3 modulate glycogen metabolism and gene transcription. Chem Biol 2000, 7:793–803
22. Summers SA, Kao AW, Kohn AD, Backus GS, Roth RA, Pessin JE, Birnbaum MJ: The role of glycogen synthase kinase 3beta in insulin-stimulated glucose metabolism. J Biol Chem 1999, 274:17934–17940
23. Kalman D, Gomperts SN, Hardy S, Kitamura M, Bishop JM: Ras family GTPases control growth of astrocyte processes. Mol Biol Cell 1999, 10:1665–1683
24. Chartier C, Degryse E, Gantzer M, Dieterle A, Pavirani A, Mehtali M: Efficient generation of recombinant adenovirus vectors by homologous recombination in Escherichia coli. J Virol 1996, 70:4805–4810
25. Barandon L, Dufourcq P, Costet P, Moreau C, Allieres C, Daret D, Dos Santos P, Daniel Lamaziere JM, Couffinhal T, Duplaa C: Involvement of FrzA/sFRP-1 and the Wnt/frizzled pathway in ischemic preconditioning. Circ Res 2005, 96:1299–1306
26. Donze O, Picard D: RNA interference in mammalian cells using siRNAs synthesized with T7 RNA polymerase. Nucleic Acids Res 2002, 30:e46
27. Couffinhal T, Kearney M, Sullivan A, Silver M, Tsurumi Y, Isner JM: Histochemical staining following Lac-Z gene transfer underestimates transfection efficiency. Hum Gene Ther 1997, 8:929–934
28. Bendeck MP, Conte M, Zhang M, Nili N, Strauss BH, Farwell SM: Doxycycline modulates smooth muscle cell growth, migration, and matrix remodeling after arterial injury. Am J Pathol 2002, 160:1089–1095
29. Huttenlocher A, Sandborg RR, Horwitz AF: Adhesion in cell migration. Curr Opin Cell Biol 1995, 7:697–706
30. Masckauchan TN, Shawber CJ, Funahashi Y, Li CM, Kitajewski J: Wnt/beta-catenin signaling induces proliferation, survival and interleukin-8 in human endothelial cells. Angiogenesis 2005, 8:43–51
31. Nobes CD, Hall A: Rho, rac, and cdc42 GTPases regulate the assembly of multimolecular focal complexes associated with actin stress fibers, lamellipodia, and filopodia. Cell 1995, 81:53–62
32. Price LS, Leng J, Schwartz MA, Bokoch GM: Activation of Rac and Cdc42 by integrins mediates cell spreading. Mol Cell Biol 1998, 9:1863–1871
33. Cattelino A, Liebner S, Gallini R, Zanetti A, Balconi G, Corsi A, Bianco P, Wolburg H, Moore R, Oreda B, Kemler R, Dejana E: The conditional inactivation of the beta-catenin gene in endothelial cells causes a defective vascular pattern and increased vascular fragility. J Cell Biol 2003, 162:1111–1122
34. Barandon L, Couffinhal T, Dufourcq P, Alzieu P, Moreau C, Daret D, Duplaa C: Exact relevance of bone marrow cells in the healing process after myocardial infarction: analysis with a murine model of bone marrow cell transplantation. Can J Cardiol 2005, 21:563–568
35. Hangai M, Moon YS, Kitaya N, Chan CK, Wu DY, Peters KG, Ryan SJ, Hinton DR: Systemically expressed soluble Tie2 inhibits intraocular neovascularization. Hum Gene Ther 2001, 12:1311–1321
36. Voskas D, Jones N, Van Slyke P, Sturk C, Chang W, Haninec A, Babichev YO, Tran J, Master Z, Chen S, Ward N, Cruz M, Jones J, Kerbel RS, Jothy S, Dagnino L, Arbiser J, Klement G, Dumont DJ: A cyclosporine-sensitive psoriasis-like disease produced in Tie2 transgenic mice. Am J Pathol 2005, 166:843–855
37. Polesskaya A, Seale P, Rudnicki MA: Wnt signaling induces the myogenic specification of resident CD45+ adult stem cells during muscle regeneration. Cell 2003, 113:841–852
38. Dennis S, Aikawa M, Szeto W, d'Amore PA, Papkoff J: A secreted frizzled related protein, FrzA, selectively associates with Wnt-1 protein and regulates wnt-1 signaling. J Cell Sci 1999, 112:3815–3820
39. Rosso SB, Sussman D, Wynshaw-Boris A, Salinas PC: Wnt signaling through Dishevelled. Rac and JNK regulates dendritic development. Nat Neurosci 2005, 8:34–42
40. Wechezak AR, Coan DE: Dvl2 silencing in postdevelopmental cells

results in aberrant cell membrane activity and actin disorganization. J Cell Physiol 2005, 202:867–873
41. Collavin L, Kirschner MW: The secreted Frizzled-related protein Sizzled functions as a negative feedback regulator of extreme ventral mesoderm. Development 2003, 130:805–816
42. Yabe T, Shimizu T, Muraoka O, Bae YK, Hirata T, Nojima H, Kawakami A, Hirano T, Hibi M: Ogon/Secreted Frizzled functions as a negative feedback regulator of Bmp signaling. Development 2003, 130:2705–2716
43. Lee JL, Lin CT, Chueh LL, Chang CJ: Autocrine/paracrine secreted Frizzled-related protein 2 induces cellular resistance to apoptosis: a possible mechanism of mammary tumorigenesis. J Biol Chem 2004, 279:14602–14609
44. Esteve P, Trousse F, Rodriguez J, Bovolenta P: SFRP1 modulates retina cell differentiation through a beta-catenin-independent mechanism. J Cell Sci 2003, 116:2471–2481
45. Le Floch N, Rivat C, De Wever O, Bruyneel E, Mareel M, Dale T, Gespach C: The proinvasive activity of Wnt-2 is mediated through a noncanonical Wnt pathway coupled to GSK-3beta and c-Jun/AP-1 signaling. FASEB J 2005, 19:144–146
46. Kim HS, Skurk C, Thomas SR, Bialik A, Suhara T, Kureishi Y, Birnbaum M, Keaney Jr JF, Walsh K: Regulation of angiogenesis by glycogen synthase kinase-3beta. J Biol Chem 2002, 277: 41888–41896
47. Rodriguez J, Esteve P, Weinl C, Ruiz JM, Fermin Y, Trousse F, Dwivedy A, Holt C, Bovolenta P: SFRP1 regulates the growth of retinal ganglion cell axons through the Fz2 receptor. Nat Neurosci 2005, 8:1301–1309
48. De Calisto J, Araya C, Marchant L, Riaz CF, Mayor R: Essential role of non-canonical Wnt signalling in neural crest migration. Development 2005, 132:2587–2597